ADVANCED MATERIALS
www.advmat.de

Large-Scale, Ultrapliable, and Free-Standing Nanomembranes

*Edward Kang, Jihee Ryoo, Gi Seok Jeong, Yoon Young Choi, Seung Min Jeong, Jongil Ju, Seok Chung, Shuichi Takayama, and Sang-Hoon Lee**

Cellular epithelia maintain their structural integrity through cell–cell and cell–extracellular matrix (ECM) adhesion. The basement membrane (BM), a thin and amorphous sheet-like structure of fibers that underlies the epithelium, plays several critical roles, including filtration and the regulation of cell proliferation, differentiation, and migration.[1–3] This membrane is positioned between epithelial cells and connective tissue, and it anatomically separates the epithelium from deeper tissues. The BM also determines the spatial relationships among various populations of cells and the space occupied by the connective and supported tissues.[4,5] Therefore, the study of cell-monolayers on the BM is critical for correct evaluation of epithelia's mechanical property in tissue. Recent technological progress based on nano- and microscale technologies has facilitated in vitro evaluation of mechanical property of epithelial or endothelial monolayer under diverse in vivo-like microenvironments,[6–10] however, most studies are limited in single or a few cells. For more in vivo mimicking study, the formation of cell monolayer on the thin BM and evaluation of its property are critical. BMs are 30–100 nanometers thick with a Young's modulus of 1–3 MPa, as summarized in Table S1. For practical usability, the membrane should be free-standing, thin and pliable comparable to BM, biocompatible, robust to handling enough to culture cells, and have a sufficiently large area (up to a few centimeters in diameter) to permit the observation and analysis of cell monolayer properties.

Several researchers have reported free-standing ultrathin (FSUT) membranes made by inorganic materials, such as silicon, metal, nanoparticles, carbon nanotubes (CNTs), or graphene.[11–15] Glucksberg et.al. have fabricated ultra-thin(UT) PDMS membranes having integrated micro/nano patterns and applied this freely suspended PDMS membrane for studying mechanical properties of very soft materials such as residual stress and young's modulus.[16] Although a few organic UT membranes have been described, most of their surface areas were less than 1 mm^2. The present paper takes this a step further, and develops a technique to fabricate large membranes and demonstrates its utility as a platform for cell study. Recently, Kunitake et al. used a spin-coating method to fabricate large UT membranes 16 cm^2 in area.[17] They subsequently developed UT membranes using a variety of materials, including zirconium oxide or thermosetting resins. Although some of these materials were organic, their utility in replacing BMs was limited because the elasticity and biocompatibility were not comparable to those of a BM. Polydimethylsiloxane (PDMS) is one of the most widely used silicon-based organic polymers, and it is broadly applied in diverse biomedical fields.[18,19] PDMS is chemically inert, biocompatible, gas permeable, and elastic. Relatively thick PDMS membranes have been used for valve, sensor, and microstructure construction.[20–23] PDMS is, therefore, a good candidate material for fabricating BM-mimicking FSUT membranes. Fabrication of large-scale FSUT PDMS membranes strong enough to culture cells, however, is still challenging due to the mechanical weakness of conventionally prepared PDMS.

In this paper, we describe the fabrication and characterization of large-scale (>2 cm in diameter) FSUT PDMS membranes and their use in investigations of mechanical property of epithelial cell monolayer on BM. The high-speed spin-coating of dilute PDMS solutions yielded FSUT membranes (<70 nm thick). Membranes were transferred to a thick PDMS ring support to facilitate easy handling. The membrane is elastic, pliable, and strong enough to endure high stretching because it is supported by ring. The pliability of the ultrathin membranes with physiological moduli were useful in cellular epithelia studies that have hitherto been impossible.

E. Kang,[+] J. Ryoo,[+] Dr. G. S. Jeong,
Y. Y. Choi, S. M. Jeong, Dr. J. Ju, Prof. S.-H. Lee
Department of Biomedical Engineering
College of Health Science
Korea University
Seoul, 136-703, Republic of Korea
E-mail: dbiomed@korea.ac.kr

Prof. S. H. Lee
KU-KIST Graduate School of Converging of Sciences & Technologies
Korea University
Seoul, 136-713, Republic of Korea

E. Kang
Department of Biomicrosystem Technology
Korea University
Seoul, 136-713, Republic of Korea

J. Ryoo
Cosmetic R&D Center
Coway Co, Seoul, 153-792, Republic of Korea

Prof. S. Chung
School of Mechanical Engineering
Korea University
Seoul, 136-713, Republic of Korea

Prof. S. Takayama
Department of Biomedical Engineering
University of Michigan
Ann Arbor, Michigan, 48109, USA

Prof. S. Takayama
Division of Nano-Bio and Chemical Engineering WCU Project
UNIST, Ulsan, 689-798, Republic of Korea

[+] These authors contributed equally to this work.

DOI: 10.1002/adma.201204619

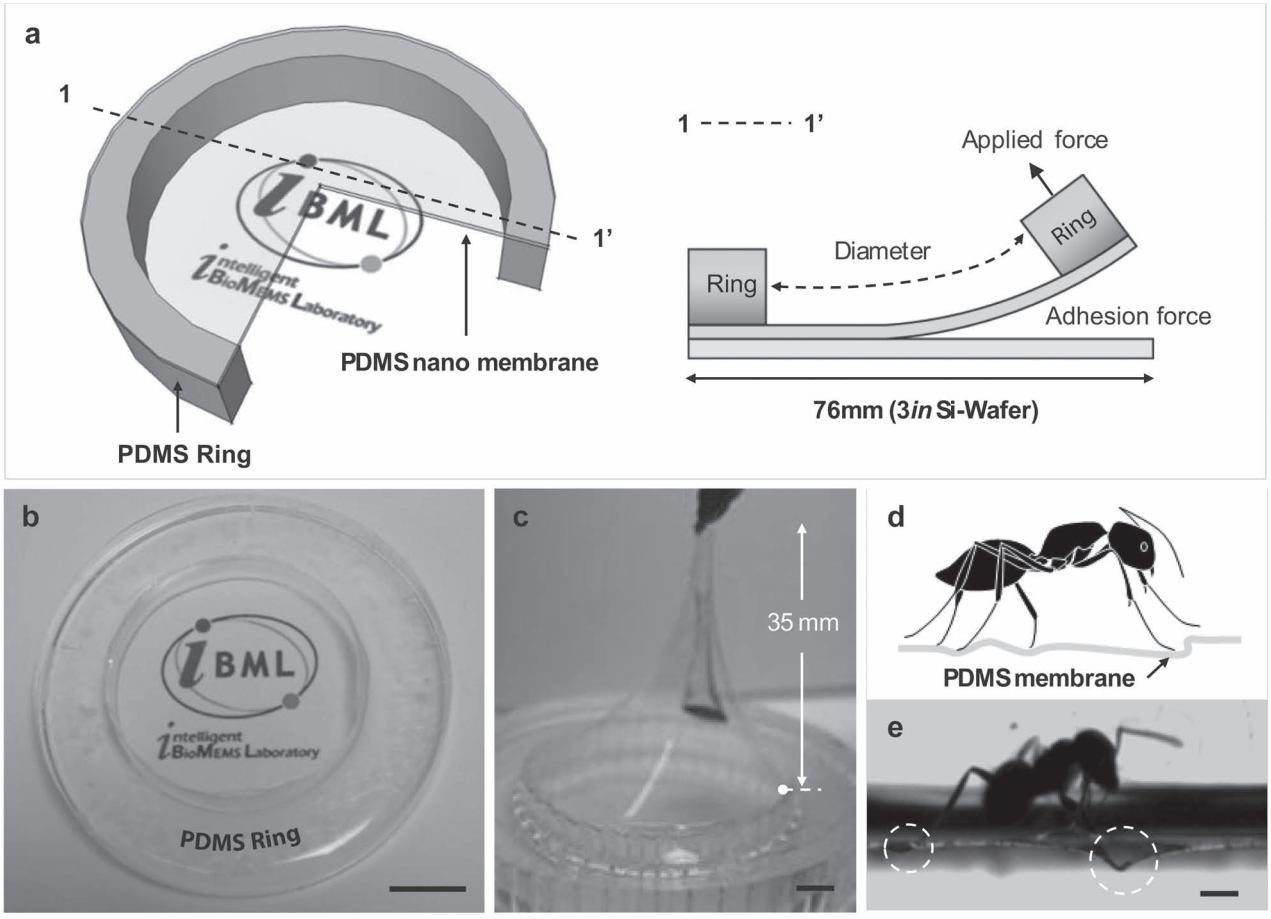

Figure 1. Fabrication of nanomembranes under shear force (a) Schematic of the PDMS nanomembrane supported by PDMS Ring. The PDMS free-standing nanomembrane was transparent, and this membrane could be fabricated on a large scale. (b) Optical image of a transparent 100 nm membrane; (c) Stretching/elongation of the membrane in the vertical direction. The stretched length was 3.5 cm. (d, e) Photograph of an ant walking on a membrane. The membrane depressed longitudinally, as captured by a CCD camera. (f) Top-view image of a PDMS nanomembrane, imaged by SEM; (g) Side-view image of a PDMS nanomembrane on an Anodisc, imaged by SEM. The scale bars indicate 10 mm in (b), 5 mm in (c,e), 500 nm in (f) and 50 nm in (g).

As shown in Figure S1(a), FSUT PDMS membranes were fabricated by spin-coating a Sylgard 184 PDMS solution diluted with hexane and deposited on a 3'' silicon wafer. A sacrificial layer (photoresist, AZ 1512) was pre-coated to a thickness of 1 μm prior to PDMS spinning to permit the easy separation of the membrane from the substrate. The spinning speed was fixed at 6000 rpm, and the thickness was determined by the dilution ratio only. The spin-coated thin PDMS membrane was transferred to a PDMS ring which played a key role to detach the FSUT membrane from the wafer without damage and to handle the membrane easily (**Figure 1**(a)). Details of the membrane detaching process are summarized in Figure S1 (b) and Video(V1). Table S2 summarizes the optimized conditions for fabricating thin membranes, including the dilution ratio and the size of the PDMS ring. The transfer of membranes thinner than 100 nm remained a challenge, and fewer than 50% of membranes survived in the transfer process. The membrane size was limited by the membrane thickness because the rate of successful transfer without failure decreased as the membrane thickness decreased. Membranes 6 cm in diameter could be detached from the substrate, provided that the minimum membrane thickness was 150 nm. In contrast, the thickness limit for a 3.5 cm diameter membrane was approximately 100 nm. A dilution ratio exceeding 1:120 (PDMS: hexane) yielded 2 cm membranes that could be successfully detached, and their thickness varied in the range of 60–80 nm. Figure 1(b) shows an optical image of an optically transparent 1:100 membrane (diameter: 3.5 cm) supported by a PDMS ring. The 1:100 PDMS membrane displayed a high elasticity, as shown in Figure 1(c). As a demonstration of the elasticity, paper tissue was adhered to the surface of the PDMS membrane, then, slowly pulled away. The attachment point of the membrane stretched upward by 3.5 cm, indicating a high elasticity, mechanical strength, and pliability of the FSUT PDMS membrane (Video(V2)). Figure 1(d) provides another demonstration of the extreme elasticity and pliability of the membrane. An ant (Lasius Niger, weight: 1.4 mg, length: ≈ 2.5 mm) was placed on the 1:100 membrane, and interestingly, the membrane under the ant's leg extended

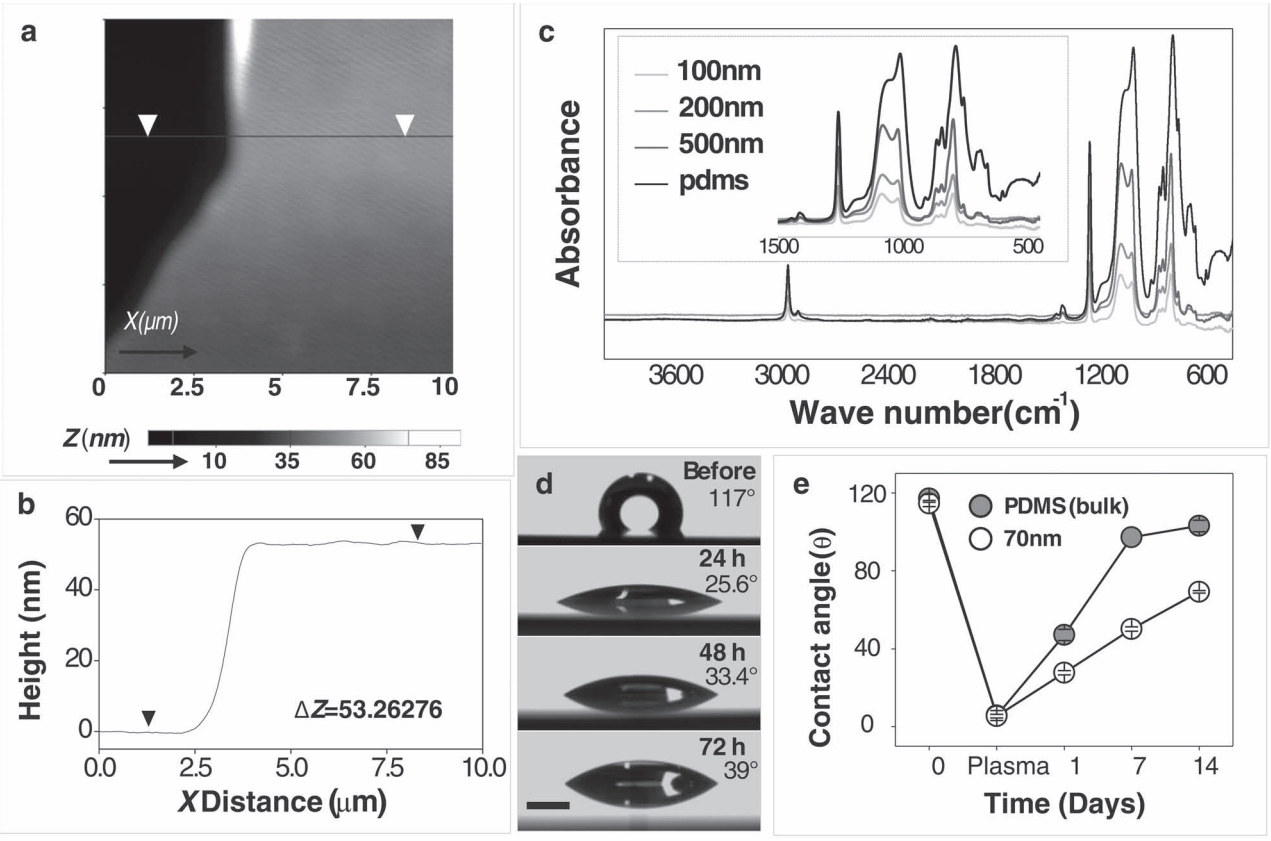

Figure 2. Characterization of a PDMS nanomembrane (a) AFM height image (Scan size 10 μm × 10 μm) of the edge of a 1:120 PDMS membrane; (b) height analysis of the profile indicated in the AFM image. A high mixing ratio yielded an ultrathin and uniform PDMS membrane. (c) ATR-FTIR spectra of the bulk PDMS, 500, 200, and 100 nm thick PDMS membranes. (d) Images of the water droplet contact angle on a 500 nm thick membrane after oxygen plasma treatment; (e) Graph of the water contact angle as a function of the aging time for PDMS membranes submitted to oxygen plasma treatment. The scale bar indicates 1 mm in (d).

partially, as indicated by the arrow in Figure 1(d, e), similar to the water surface deformation observed under a water strider (Video(V3)). For better visualization, FSUT PDMS membranes were transferred to porous alumina discs (Anodisc 25, Whatman International Ltd). Figure 1(f) shows a top-view SEM image of the membrane on the alumina disc (mean pore size: 100–150 nm). The porous area indicates the surface of the disc, and the nanomembrane covered half of the porous disc without producing any defects or cracks. A cross-sectional scanning electron microscopy (SEM) image of the nanomembrane allowed direct measurement of the membrane thickness (Figure 1(g)). The surface profile of the FSUT membrane was varied by a few nanometers along the porous disc, indicating its ultra-pliability. The measured minimum thickness was 33.1 nm, and the average thickness was 50–60 nm, which differed slightly from the thickness measured by atomic force microscopy (AFM). These FSUT membranes were strong enough to endure high extensions because the long PDMS polymer chains (0.7 nm in diameter) which is coiled like tangled spaghetti were stretched by the high shear stress.[24]

All thickness values were measured using AFM, and 6–10 samples per each dilution ratio were prepared for each case (Figure S2). The fabrication processes were carried out in a clean room with control over the temperature and humidity. At a 1:40 dilution ratio, the membrane thickness was 350 nm, and the thickness decreased logarithmically. The thickness decreased to approximately 70 nm for a dilution ratio of 1:120. As the dilution ratio decreased below 1:120, the success rate of separation was less than 30%. **Figure 2**(a) displays a large-scale (10 μm × 10 μm) topographic AFM image of the edge of a 1:120 PDMS membrane. The height of membrane between arrows was measured, and Figure 2(b) illustrates the corresponding height profile. To measure the height, the specimen on the wafer was locally scratched with a sharp needle to create an edge. The surface profile of the membrane was smooth and the thickness was constant within an accuracy of 99% over the whole membrane, indicating the silica fillers in Sylgard 184 PDMS are homogeneously distributed.[25] The curing temperature was 80 °C, and the curing time exceeded 6 hours. The membranes became more stable and provided higher rates of transfer success with increased curing times (>6 hr). We investigated whether the chemical composition of the membrane was the same as that of the bulk PDMS using ATR-FTIR spectroscopy. As illustrated in Figure 2(c), no significant differences were observed between the thin and bulk PDMS, which indicated that the chemical properties of PDMS were not affected

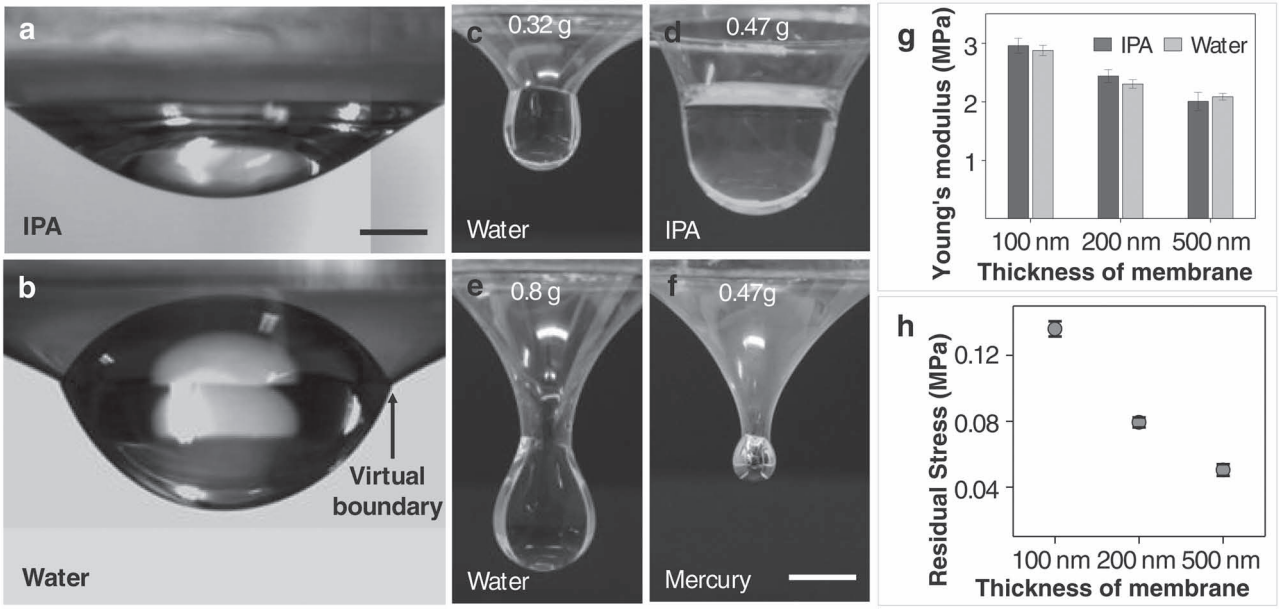

Figure 3. Mechanical properties of a PDMS nanomembrane (a, b) Images of an 80 µL droplet on the membrane, IPA, water respectively; (c-f) Side-view optical images of a membrane extended under the weight of different liquids: (c, e) water, (d) IPA, (f) mercury; (g) Young's modulus of the membranes with different thicknesses under the weight of water or IPA. (h) Residual stresses as a function of thickness under the weight of IPA. The scale bars indicate 1 mm in (a) and 5 mm in (f).

by the dilution and thinning processes. The surface properties of the thin membrane were analyzed using a goniometer. Prior to oxygen plasma treatment, the water contact angles of all samples ranged from 108° to 119°, and no significant differences were observed relative to the water contact angle of the bulk PDMS (115°). Immediately after oxygen plasma treatment, all samples displayed hydrophilic surface properties. A photograph of a droplet on the 500 nm membrane is presented in Figure 2(d) (70 nm membrane and bulk PDMS: Figure S3(a)), and the contact angles measured over 14 days of recovery for all samples, after plasma exposure, are plotted in Figure 2(e) and Figure S3(b). The bulk PDMS surface recovered its original hydrophobic properties, but the recovery angle for the nanomembranes was much lower than that of the bulk PDMS. Hydrophobic recovery after plasma treatment results from the migration of uncured PDMS oligomers from the bulk to the surface.[26] The slower and lower hydrophobic recovery properties may indicate less migration of the uncured PDMS oligomers or other unknown factors.

The thin PDMS membrane was ultra-elastic and displayed the ultra-pliable properties of larger solid membranes. Two types of liquid (water and isopropyl alcohol (IPA), 80 µL each) were dropped onto a 70 nm thick membrane, and the membrane extension was monitored (**Figure 3**(a) and Figure 3(b)). Water droplets beaded up and locally deformed the membranes due to the high surface tension and contact angle (Figure S4). As the volume of water increased, the membrane underlying the droplet extended anisotropically to form a pendant droplet under the force of gravity (Figure 3(c), Video(V4)). In contrast, the lower surface tension and lower contact angle of the IPA extended the membrane isotropically (Figure 3(d)). Figure 3(e) and Figure 3(f) show images of the 70 nm membrane extension under 0.8 g water or 0.47 g mercury. As the density and surface tension of the liquid increased, the anisotropic extension toward the gravitational direction increased, and the curvature of the extended membrane became sharper. The modulus of the nanomembrane was calculated by measuring the extension of the membrane (Figure S5). The modulus of a 70 nm thick membrane was 50% larger than the modulus of a 500 nm thick membrane (Figure 3(g)), which was slightly larger than the modulus of a 30 µm thick membrane. The modulus of the 30 µm thick membrane was measured using an ASTMD 412 test.[27] We further calculated the residual stresses as a function of thickness and the result is plotted in Figure 3(h).[16] The higher moduli of the thinner membranes are attributed, at least in part, to the polymer strand stretching during the spin coating process.[27] Plasma treatments alter the wetting and mechanical properties of ultra-thin membranes. After plasma exposure onto membrane surface, the residual stress and young's modulus of nanomembrane were calculated by measuring the extension of the membrane (Figure S4(c)). As the exposure time of plasma increased, the length of curvature of the membrane became reduced, which indicated that the plasma treatment increase the stiffness of membrane compared to non-treated membrane.

The ability to analyze the mechanical properties of epithelia on BM is important in understanding organogenesis and tissue homeostasis.[28] Taking advantage of the FSUT membrane, we directly measured the modulus of an epithelia layer formed by a kidney cell line. In this procedure, MDCK cells (density: 2×10^4) were seeded (**Figure 4**(a) upper and Figure 4(b)) and cultured to confluence (Figure 4(c)) on 70 and 500 nm thick membranes over 3 days. These epithelia formed nice cell–cell junctions, as

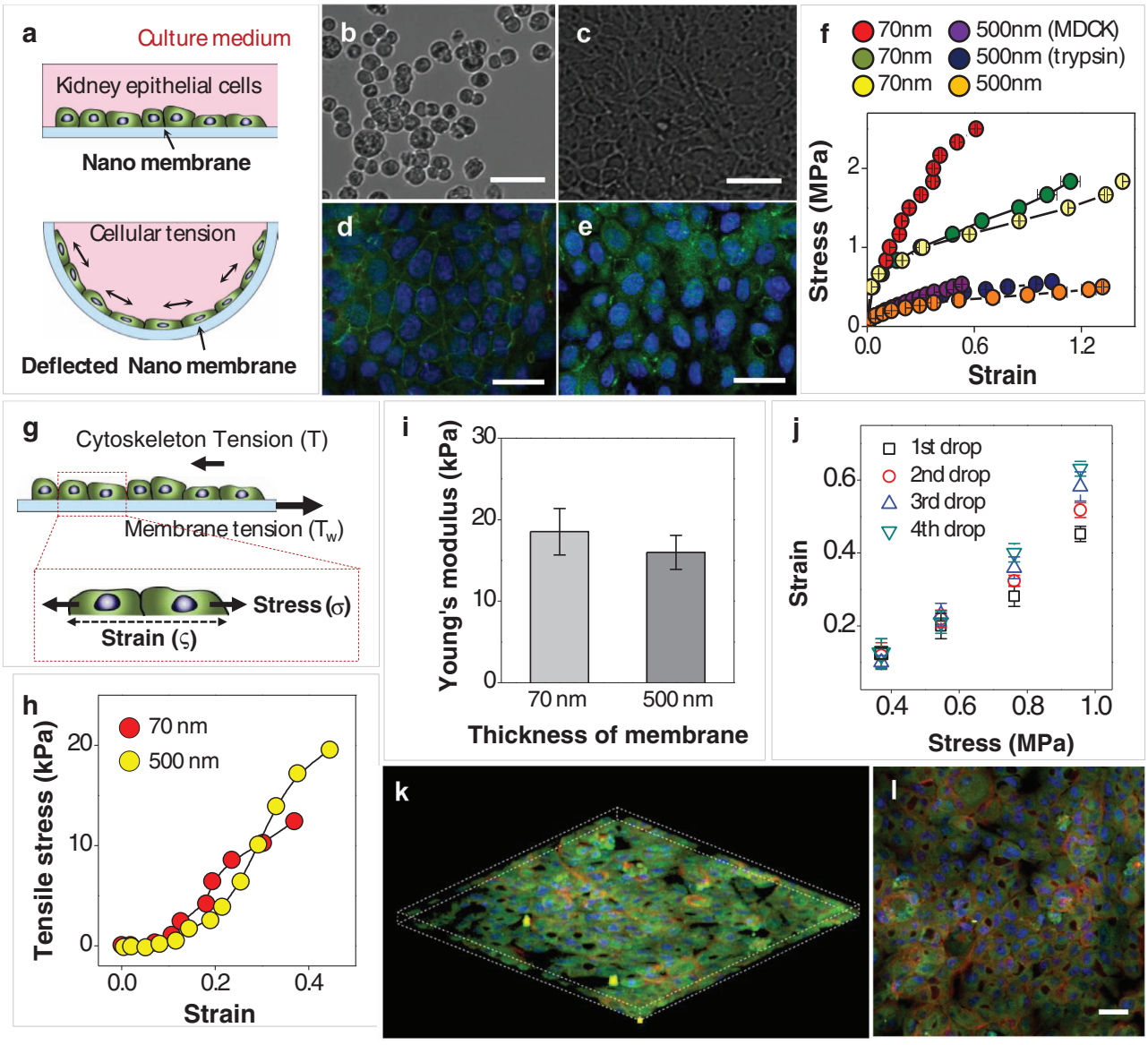

Figure 4. Mechanical properties of cell–monolayer (a) A schematic diagram of the MDCK cell monolayer on a membrane (top) and on a deflected membrane (bottom); (b) Phase contrast images of MDCK cells after seeding and (c) after 3 days (scale bar: 50 μm); (d) Staining image of the tight cell junctions on the nanomembrane; (e) Fluorescent image of the damaged cell junctions after a large deflection (80% stretching test); (f) Stress–strain curves for a bare membrane, a cell monolayered membrane, and a trypsin-treated membrane (thickness: 70 nm or 500 nm); (g) 2D schematic diagram showing the monolayer thickness at the cell–cell junctions and at the center of a cell; (h) tensile stress and strain for a cell monolayer derived from the difference between the bare and monolayered membrane; (i) Young's modulus of an MDCK cell–monolayer; (j) plot of the strain–stress curves for repeated 10%, 20%, 30% and 40% stretching tests of a cell monolayer grown on a 100 nm thick membrane. (k) 3D confocal image and (l) confocal overlay image of a MDCK cell monolayer undamaged by water force (initial strain 20%). The scale bars indicate 50 mm in (b,c), 25 μm in (d,e) and 15 μm in (l).

visualized using anti-ZO-3(green) staining (Figure 4(d)). These junctions became disrupted after subjection to 20 minutes of an 80% stretched state Figure 4(e). The modulus of epithelia monolayer was analyzed in detail by subjecting the constructs to a defined stress by dropping defined volumes of cell culture media onto the membranes and measuring the deflection to obtain strain. Figure 4(f) shows the stress–strain curve for a bare membrane without cells, a membrane with a confluent cell monolayer, and a membrane with cell monolayers that had been trypsin-treated to disrupt the cell–cell and cell–ECM interactions. As expected, the deflection of the membrane was affected by the cell–monolayer spread on the membrane (Figure 4(g)). The 70 nm thick membrane deflected more than the 500 nm thick membrane. After treatment with trypsin, the mechanical effects of the cell monolayer disappeared for both the 70 and 500 nm thick membranes. By subtracting the mechanical response of the bare FSUT membrane, the modulus of the living cell monolayer was obtained (Figure 4(h)). Figure S6(c)

shows the strain-stress curve of cell monolayer at the lower strain range, and even at this range, strain of cell monolayer is sensitively changed. The Young's modulus of the intact cell monolayer itself, irrespective of the thickness of the membrane on which the cells were cultured, was ~20 kPa (Figure 4(i)). This may be the first direct measurement of the modulus of a cell monolayer. We further performed 10, 20, 30 and 40% cyclic stretching tests using the 100 nm thick membrane where the stretching was repeated 4 times (Figure 4(j)). Under 10% and 20% stretching conditions, the stress-strain relation of the cell monolayer membrane remained unchanged over the 4 stretches (3D Confocal image in Figure 4(k-l)), indicating that the cell–cell tight junctions in the continuous tissue were preserved. The 30 and 40% stretching conditions led to gradual change in the stress-strain relation, suggesting that the junctions were degraded as stretching was repeated. The ability to measure the modulus of cell monolayers directly provides new opportunities for monitoring epithelial function and structure non-invasively and in near real-time. As the epithelia and endothelia in many organs are exposed to physiological stretching under normal and diseased conditions, this capability should be broadly useful for studies of many cellular systems.

In summary, we describe an optimized method for fabricating large-area FSUT PDMS membranes, and we characterized several properties of the membrane, particularly its high pliability. To our knowledge, such large-area, highly pliable, and biocompatible FSUT membranes are unprecedented. We also demonstrated the use of these membranes for analyzing mechanical property of epithelia. The FSUT membrane–cell models open new opportunities to enhance our understanding of mechanical cell injury, and mechanotransduction to the extent that such factors can contribute to disease treatment and tissue engineering. The ultra-pliability of the membrane may also be useful in non-cellular applications, such as the construction of highly sensitive sensors for measuring pressures, magnetic forces, or biochemical interactions, by integrating the membranes with appropriate metals, magnets, or biological materials.

Experimental Section

Materials: Hexane (mixture of isomers - ACS reagent, ≥ 98.5%) and PDMS (Sylgard184) were purchased from Sigma-Aldrich and Dow Corning, respectively. AZ1512 (photoresist) was obtained from AZ Electronic Materials. Anodisc25 (pore size ~ 0.15 μm, diameter 20 mm) was purchased from Whatman International Ltd. The PTFE Syringe filters (0.45 μm, diameter 13 mm) were purchased from Whatman Schleicher & Schuell.

Fabrication of free-standing PDMS nanomembranes: The fabrication of ultrathin (UT) (< 70 nm) PDMS nanomembranes was carried out as follows (Figure S1(a)). First, a 1 μm thick sacrificial layer of AZ1512 was spin-coated onto a clear silicon wafer. Because small particles affect the production of the membrane, the silicon wafer should be kept clean. Secondly, PDMS solutions were diluted with hexane prior to spin-coating. The ratio of hexane to PDMS (wt%) was an important factor that controlled the membrane thickness. A PDMS prepolymer to curing agent ratio of 10:1 was used. Prior to spin-coating, impurities were filtered from the hexane–PDMS solution using a glass syringe with a PTFE syringe filter. The PDMS-hexane solution (800 μL) was spin-coated onto a sacrificial layer at 6000 RPM for 3 min. At least 12 hours curing time and 80 °C temperatures were required for curing on the hotplate. The PDMS block (diameter >2 cm, height >5 mm) was bonded using an intermediate pre-polymerized PDMS, then cured for 2 hours on a hotplate (Figure S1(b, left)). The next step was detachment. Acetone was spread across the membrane surface only within the PDMS block area (Figure S1 (b, right-i)). Spreading the acetone on the membrane partially dissolved the sacrificial layer and enabled the smooth detachment of the PDMS nanomembrane in methanol (Figure S1 (b, right-ii)). The membrane was shaken in methanol then carefully removed (Figure S1 (b, right-iii)). The hexane–PDMS membrane is shown in Figure S1 (b, right-iv). After detachment, the wafer was cleaned using two methods: piranha cleaning, which can be used to prepare a wafer for reuse after the fabrication process, and chemical washing, which involves washing the wafer with acetone, methanol, and IPA, sequentially. Acetone, methanol, and IPA were spread across the wafer to remove the AZ1512 and PDMS residues. The wafer was then blow-dried using a nitrogen gun.

Supporting Information

Supporting Information is available from the Wiley Online Library or from the author.

Acknowledgements

This study was supported by the National Research Foundation of Korea(NRF) grant funded by the Korea government(MEST), Republic of Korea (No. 2012026340) and the Converging Research Center Program funded by the Ministry of Education, Science and Technology (2012K001360), and S. Takayama thanks the NRF-WCU program funded by MEST (R322008000200540).

Received: November 7, 2012
Revised: December 18, 2012
Published online: February 19, 2013

[1] S. E. Bell, A. Mavila, R. Salazar, K. J. Bayless, S. Kanagala, S. A. Maxwell, G. E. Davis, *J. Cell Sci.* **2001**, *114*, 2755.
[2] R. Kalluri, *Nat. Rev. Cancer* **2003**, *3*, 422.
[3] D. Q. Matus, X. Y. Li, S. Durbin, D. Agarwal, Q. Y. Chi, S. J. Weiss, D. R. Sherwood, *Sci. Signal* **2010**, *3*.
[4] L. S. Fujikawa, C. S. Foster, I. K. Gipson, R. B. Colvin, *J. Cell Biol.* **1984**, *98*, 128.
[5] D. R. Sherwood, *Trends Cell Biol.* **2006**, *16*, 250.
[6] J. Y. Park, S. Takayama, S. H. Lee, *Integr. Biol. - UK* **2010**, *2*, 229.
[7] D. Huh, G. A. Hamilton, D. E. Ingber, *Trends Cell Biol.* **2011**, *21*, 745.
[8] C. S. Chen, M. Mrksich, S. Huang, G. M. Whitesides, D. E. Ingber, *Science* **1997**, *276*, 1425.
[9] D. B. Weibel, W. R. DiLuzio, G. M. Whitesides, *Nat. Rev. Microbiol.* **2007**, *5*, 209.
[10] A. Khademhosseini, R. Langer, J. Borenstein, J. P. Vacanti, *Proc. Natl. Acad. Sci. USA* **2006**, *103*, 2480.
[11] C. Lee, X. D. Wei, J. W. Kysar, J. Hone, *Science* **2008**, *321*, 385.
[12] K. S. Kim, Y. Zhao, H. Jang, S. Y. Lee, J. M. Kim, K. S. Kim, J. H. Ahn, P. Kim, J. Y. Choi, B. H. Hong, *Nature* **2009**, *457*, 706.
[13] K. E. Mueggenburg, X. M. Lin, R. H. Goldsmith, H. M. Jaeger, *Nat. Mater.* **2007**, *6*, 656.
[14] J. A. Rogers, M. G. Lagally, R. G. Nuzzo, *Nature* **2011**, *477*, 45.
[15] C. C. Striemer, T. R. Gaborski, J. L. McGrath, P. M. Fauchet, *Nature* **2007**, *445*, 749.
[16] A. L. Thangawng, R. S. Ruoff, M. A. Swartz, M. R. Glucksberg, *Biomed. Microdev.* **2007**, *9*, 587.
[17] R. Vendamme, S. Y. Onoue, A. Nakao, T. Kunitake, *Nat. Mater.* **2006**, *5*, 494.

[18] D. J. Beebe, G. A. Mensing, G. M. Walker, *Annu. Rev. Biomed. Eng.* **2002**, *4*, 261.
[19] W. F. Liu, C. S. Chen, *Mater. Today* **2005**, *8*, 28.
[20] E. Kang, G. S. Jeong, Y. Y. Choi, K. H. Lee, A. Khademhosseini, S. H. Lee, *Nat. Mater.* **2011**, *10*, 877.
[21] M. Cha, J. Shin, J. H. Kim, I. Kim, J. Choi, N. Lee, B. G. Kim, J. Lee, *Lab Chip* **2008**, *8*, 932.
[22] D. J. Lipomi, M. Vosgueritchian, B. C. K. Tee, S. L. Hellstrom, J. A. Lee, C. H. Fox, Z. Bao, *Nat. Nanotechnol.* **2011**, *6*, 788.
[23] D. H. Lee, J. Y. Park, E. J. Lee, Y. Y. Choi, G. H. Kwon, B. M. Kim, S. H. Lee, *Biomed. Microdev.* **2010**, *12*, 49.
[24] S. Granick, Z. Q. Lin, S. C. Bae, *Nature* **2003**, *425*, 467.
[25] A. Olah, H. Hillborg, G. J. Vansco, *Appl. Surf. Sci.* **2005**, *239*, 410.
[26] A. Toth, I. Bertoti, M. Blazso, G. Banhegyi, A. Bognar, P. Szaplonczay, *J. Appl. Polym. Sci.* **1994**, *52*, 1293.
[27] M. Liu, J. R. Sun, Y. Sun, C. Bock, Q. F. Chen, *J. Micromech. Microeng.* **2009**, *19*.
[28] J. D. Humphrey, *Proc. R. Soc. A - Math. Phys.* **2003**, *459*, 3.